Thermal behavior of buildings with curved roofs as compared with flat roofs

Article *in* Solar Energy · April 2003
DOI: 10.1016/S0038-092X(03)00193-2

3 authors, including:

Runsheng Tang
Yunnan Normal University
59 PUBLICATIONS **1,084** CITATIONS
SEE PROFILE

Isaac A Meir
Ben-Gurion University of the Negev
76 PUBLICATIONS **733** CITATIONS
SEE PROFILE

Available online at www.sciencedirect.com
SCIENCE DIRECT®
Solar Energy 74 (2003) 273–286
SOLAR ENERGY

Thermal behavior of buildings with curved roofs as compared with flat roofs

Runsheng Tang*, I.A. Meir[1], Y. Etzion[1]

Desert Architecture and Urban Planning Unit, Department for Man in Drylands, J. Blaustein Institute for Desert Research, Ben-Gurion University of the Negev, Sede Boqer Campus 84990, Israel

Received 28 October 2002; received in revised form 5 May 2003; accepted 7 May 2003

Abstract

In this paper, a detailed finite element model dealing with heat transfer through a domed or vaulted roof is suggested based on a three-dimensional heat transfer equation and solar geometry. This model allows a comparison of the thermal behavior of curved and flat roofs in terms of heat flux and daily heat flow through them into an air-conditioned building under different climatic conditions. The results of numerical calculations show that the ratio of daily heat flow through curved roofs to that through flat ones is not affected by the curve radius, thickness and construction material of the roof, but is significantly influenced by the half rim angle θ_0 of the roofs and the ambient temperature. Compared to a flat roof, under typical hot dry climatic conditions, the daily heat flow through a domed roof of $\theta_0 = 90°$ is about 40% higher, whereas the daily heat flow through a south–north oriented and an east–west oriented vault of $\theta_0 = 90°$ is about 20 and 27% higher, respectively. The reason for this is mainly attributed to the convective heat transfer between the enlarged curved roof and ambient air. However, when $\theta_0 < 50°$, heat flux and daily heat flow through a curved roof is close to that through a flat roof. The results also confirm that curved roofs are not suitable for areas with higher air temperature and intense sky diffuse radiation typical of hot humid areas.

1. Introduction

Domed and vaulted roofs have been extensively used in traditional vernacular buildings in hot dry regions. Such roofs were commonly constructed using stone or brick masonry with a plaster finish (Fig. 1). Usually, a small opening close to the top of the gable walls of the vaults provides ventilation and exhausts hot air from the upper strata. Since wood is scarce in such regions, the construction materials commonly used are stone or mud. These have dictated roof forms based on the geometry and morphology of arch, vault and dome. Climate-related explanations given for curved roofs have been investigated by many researchers. Some researchers have assumed that these roofs were adopted out of climatic and environmental considerations, while others stressed religious and cultural issues of geometry. Common among these explanations was the assumption that, in hot dry climates, buildings with curved roofs maintain lower indoor temperatures during the hot summer months and reflect more radiation than flat roofs (Fathy, 1973; Mainstone, 1983; Bowen, 1981; Koita, 1981). The reason for this assumption was mainly qualitative, based on the assessed interaction between desert climate and the enlarged curved roof surface as compared to flat roofs. Olgyay (1973) and Fathy (1986) suggested that an advantage of curved roofs was that they reduced local radiant flux on a rounded surface and therefore resulted in lower surface temperatures, so the heat flowing into buildings through curved roofs was also reduced. This explanation, in fact, was incomplete since the lower roof temperature will cause less heat dispersion by thermal radiation and convection, thus the net solar heat flowing into buildings through curved roofs was not reasonably proved to be reduced. Another explanation given for the abundance of curved roofs in hot arid regions

*Corresponding author. Tel.: +972-8-659-6875; fax: +972-8-659-6881. Present address: Solar Energy Research Institute, Yunnon Normal University, Kunming 650092, P.R. China. Tel.: +86-871-5151719.

E-mail address: runsheng@bgumail.bgu.ac.il (R. Tang).

[1]Member of ISES.

0038-092X/03/$ – see front matter
doi:10.1016/S0038-092X(03)00193-2

Nomenclature

A	area of roof base (m^2)
C_p	specific heat (J kg^{-1} K^{-1})
d	thickness of the roof (m)
f_x	control function, either 0 or 1
h	heat transfer coefficient between roof and air (W m^{-2} K^{-1})
I	solar intensity (W m^{-2})
k	thermal conductivity (W m^{-1} K^{-1})
$\boldsymbol{n}$	unit vector
Q	daily heat flow through roof (J m^{-2})
q	heat flux through roof (W m^{-2})
R	radius of curved roof (m)
r	radial coordinate (m)
Rh	relative humidity of air (%)
S	solar heat gain of roof (W m^{-2})
T	temperature (°C)
t	time
x	coordinate from the external surface of a flat roof
α	absorptance of roof
δ	declination of the sun (deg)
ε	emittance of roof
ϕ	azimuth angle (deg)
ϕ_v	orientation of vaults, from due south to west (deg)
λ	local latitude (deg)
μ	thermal diffusivity of roof (10^{-6} m^2 s^{-1})
θ	polar angle from zenith (deg)
θ_0	half rim angle of both dome and vault (deg)
ρ	density of roof (kg m^{-3})
ρ_g	reflectance of ground
σ	Stefan–Boltzmann constant (W m^2 K^4)
ω	hour angle from solar noon to afternoon (deg)

Subscripts

a	ambient air
b	beam radiation
d	domed roof, diffuse radiation
dp	dew point
ex	external surface of roofs
f	flat roof
h	horizontal
i	indoor air, incidence angle
in	internal surface of roofs
n	normal
s	solar ray
sky	sky
t	top element within $\theta \leq \theta_c$
v	vaulted roof
z	zenith

was that these absorb the same amount of radiation as compared with flat roofs, but dissipate more heat by convection. Due to thermal stratification, the air heated within a building with a curved roof gathers in the space under the roof, thus creating more comfortable conditions on the living/floor level (Koita, 1981; Bahadori, 1978). This interpretation sounds logical, but the idea of more heat dissipated by curved roofs by convection has been

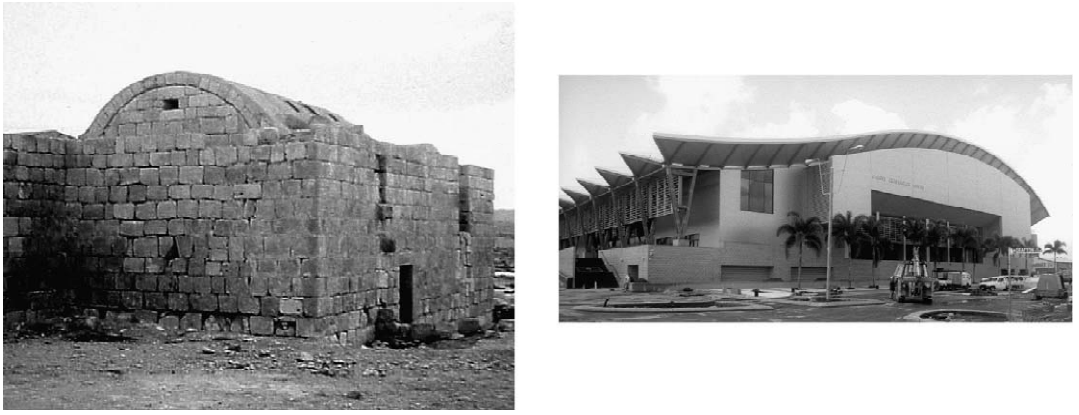

Fig. 1. Left: bathhouse stone vault, ca. 1–5 c.CE, Avdat, hot dry Israeli desert. Right: vaulted roof, conventions center, Cairns, hot humid Australian north.

shown to be unsubstantiated, since ambient temperature outside the building is often higher than that of indoor air during the daytime, hence more heat would be transferred by convection into buildings through the enlarged curved roofs. Nevertheless, contemporary architecture adopted such roof forms without questioning the ''common knowledge'' on their thermal properties and behavior.

Pearlmutter (1993) made a first attempt to quantitatively compare the thermal behavior of vaulted and flat roofs in terms of indoor temperatures. Two pairs of test structures were constructed, each of the pairs consisting of one structure with a flat roof and one with a semi-cylindrical roof. The roofs of one pair were painted black matte, and those of the other pair were painted white. Roofs were made of 1 mm thick galvanized sheet metal, and the walls and floors were constructed of plywood with 5 cm expanded polystyrene insulation. Each structure measured 50 cm × 50 cm in plan, and 50 cm in height from the floor to the base of the roof. Pearlmutter found no significant difference between the thermal conditions of the south–north facing vaulted roofs and the east–west facing ones (the central axial line of the vault oriented parallel to the south–north direction for an east–west facing vaulted roof); thermal stratification under vaulted roofs was found to be higher than that under flat ones; the roof geometry affected average indoor air temperatures over the daily cycle were altered by less than 1 °C, with the vault's average being slightly lower when painted black and slightly higher when painted white.

Theoretical calculations of solar gains absorbed by vaulted roofs compared with flat roofs were also performed based on solar geometry. However, a sensitivity analysis of the solar heat gains of vaulted roofs to their structural parameters was not performed. Such work was recently undertaken by Tang et al. (2003) based on solar geometry and the angular-dependent solar absorptance of surfaces. This research showed that a domed roof with a half rim angle of 90° absorbs 20% more beam radiation, 50% more sky diffuse radiation, and 30% more total radiation (not including ground reflected radiation) than that received by a flat roof. It also showed that a south–north facing vaulted roof with a half rim angle of 90° absorbs almost the same amount of beam radiation, 28.5% more sky diffuse radiation, and 10% more total radiation compared to flat roofs. The same study also showed that the ratio of radiation absorbed by curved roofs to that absorbed by flat ones increases with increasing half rim angle, but is insignificantly affected by climate characteristics and site latitude. Furthermore, it was demonstrated that a south–north facing vaulted roof is advantageous in reducing solar heat gains during summer months and increasing solar heat gains during winter months compared to an east–west facing one.

In this paper, a first attempt is made to calculate the heat flux and the daily heat flow through curved roofs into an air-conditioned building based on solar geometry and a three-dimensional equation of unsteady heat transfer. This allows the assessment of the energy efficiency of this building type regarding cooling loads under hot arid climatic conditions. The aim of this exercise was to investigate the energy implications of the adoption by modern architecture of traditional building technologies, forms and elements.

2. Mathematical model

To investigate the heat flux through curved roofs into the interior of an air-conditioned building as compared to buildings with flat roofs, it is assumed that the curved roofs are of identical properties to the flat roofs, built with thickness d, base area A, and the same construction material; no heat transfer takes place between the curved roof and its base walls; no heat is generated inside the

buildings; the thermal properties of the construction material do not change with temperature. The heat flux through curved roofs is calculated on the basis of the base area A, instead of the curved surface area.

2.1. Heat transfer through a domed roof (DR)

Assuming the DR in discussion is constructed of a homogeneous construction material with average radius R, half rim angle θ_0 (see Fig. 2), the outer radius of the roof is $r_{ex} = R + 0.5d$, the inner radius is $r_{in} = R - 0.5d$, and the area of the roof base is $A = \pi R^2 \sin^2\theta_0$. In the spherical coordinate system, the heat transfer of a DR can be expressed by (Incropera and Dewitt, 1996)

$$\frac{1}{r^2}\frac{\partial}{\partial r}\left(kr^2\frac{\partial T}{\partial r}\right) + \frac{1}{r^2\sin^2\theta}\frac{\partial}{\partial \phi}\left(k\frac{\partial T}{\partial \phi}\right) + \frac{1}{r^2\sin\theta}\frac{\partial}{\partial \theta}\left(k\sin\theta\frac{\partial T}{\partial \theta}\right) = \rho C_p\frac{\partial T}{\partial t} \quad (1)$$

The boundary conditions of the above equation are given by

$$-k\frac{\partial T}{\partial r}\bigg|_{r=r_{ex}} = S - h_{ex}(T_{ex} - T_a) - 0.5\varepsilon\sigma[(T_{ex}+273)^4 - T_{sky}^4](1+\cos\theta) \quad (2)$$

$$-k\frac{\partial T}{\partial r}\bigg|_{r=r_{in}} = -h_{in}(T_{in} - T_i) \quad (3)$$

$$\frac{\partial T}{\partial \theta}\bigg|_{\theta=\theta_0} = 0 \quad (4)$$

$$\frac{\partial T}{\partial \theta}\bigg|_{\theta\le\theta_c} = \frac{\partial T}{\partial \phi}\bigg|_{\theta\le\theta_c} = 0 \quad (5)$$

The initial condition is given by

$$T(\theta,\phi,r,t)|_{t=0} = T_i \quad (6)$$

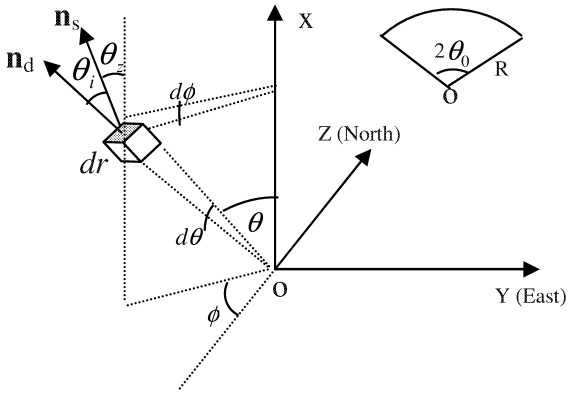

Fig. 2. Solar ray vector $\boldsymbol{n}_s$ and normal vector $\boldsymbol{n}_d$ at any point of a domed roof (DR).

The boundary condition given by Eq. (5) is based on the assumption that the temperature at the top of the DR within $\theta \le \theta_c$ (θ_c is small, e.g. 5°) only depends upon the radial coordinate, r, and time, t, i.e. the temperature within this part of the roof is uniform (just like in a flat roof) for a given moment on a given layer of the DR. T_{sky}, the equivalent sky temperature in degrees Kelvin, is determined for a clear sky by the procedure presented by Berdahl and Fromberg (1982):

$$T_{sky} = \varepsilon_{sky}^{0.25}(T_a + 273) \quad (7)$$

$$\varepsilon_{sky} = 0.74 + 0.006T_{dp} \quad (8)$$

For moist air, the dew point temperature T_{dp}, ranging from 0 to 65 °C, has the following empirical correlation expressed in degrees Celsius (Cook, 1985):

$$T_{dp} = 26.14 + 16.99c + 1.8893c^2 \quad (9)$$

According to the definition of the dew point temperature, the reversed formula of Eq. (9) can be used to calculate the saturation vapor pressure P_a of the air at any air temperature, hence

$$c = \ln(Rh \times P_a) = \ln(Rh) - 8.0929 + 0.97608(T_a + 42.607)^{0.5} \quad (10)$$

In Eq. (2), S is the radiation absorbed per unit area of the DR at any point as a function of time, t, polar angle, θ, and azimuth angle, ϕ. To simplify the calculation of S, we suggest such a coordinate system that its origin is located at the center of the dome with the Y-axis pointing due east and the Z-axis pointing due north, as shown in Fig. 2. Thus, at any given time, the beam radiation absorbed per unit area at any point of the DR would be given by

$$S_b = f_x I_b \cos\theta_i \alpha(\theta_i) \quad (11)$$

where $\alpha(\theta_i)$ is the solar absorptance of the external surface of the DR as a function of the solar incidence angle, θ_i. A correlation recommended by Duffie and Beckman (1991) was adopted in this study as follows:

$$\alpha(\theta_i)/\alpha_n = 1 + 2.0345\times10^{-3}\theta_i - 1.99\times10^{-4}\theta_i^2 + 5.324\times10^{-6}\theta_i^3 - 4.799\times10^{-8}\theta_i^4 \quad (0 \le \theta_i \le 80°) \quad (12a)$$

$$\alpha(\theta_i)/\alpha_n = 0.064938(90 - \theta_i) \quad (80 < \theta_i < 90°) \quad (12b)$$

For sky diffuse radiation and reflected radiation from the ground, assuming their distribution is isotropic over the hemisphere above a horizontal surface, the corresponding equivalent absorptance α_d of a surface can be estimated by integrating $\alpha(\theta_i)$ over the hemisphere as follows:

$$\alpha_d = \int_0^{90} 2 \sin\theta_i \cos\theta_i \alpha(\theta_i)\, d\theta_i = 0.93335\alpha_n \quad (13)$$

In Eq. (11), $\cos\theta_i$ is determined using the dot product between the unit normal vector $\boldsymbol{n}_d$ at any point of the DR and the unit solar ray vector $\boldsymbol{n}_s$, i.e.

$$\cos\theta_i = \boldsymbol{n}_d \cdot \boldsymbol{n}_s \quad (14)$$

In the suggested coordinate system, vectors $\boldsymbol{n}_s$ and $\boldsymbol{n}_d$ would be expressed by (Rabl, 1985)

$$\boldsymbol{n}_s = (\cos\theta_z,\ -\cos\delta \sin\omega,\ -\cos\delta \cos\omega \sin\lambda + \sin\delta \cos\lambda) \quad (15)$$

$$\boldsymbol{n}_d = (\cos\theta,\ -\sin\theta \sin\phi,\ -\sin\theta \cos\phi) \quad (16)$$

where θ_z is the zenith angle of the sun, and is determined by

$$\cos\theta_z = \cos\delta \cos\omega \cos\lambda + \sin\delta \sin\lambda \quad (17)$$

f_x in Eq. (11) is a control function, being 0 when $\cos\theta_i < 0$, meaning that no beam radiation strikes at this point in this case; otherwise, f_x equals 1. The diffuse radiation, S_d, absorbed per unit area at any point of the DR is expressed by

$$S_d = \alpha_d[0.5I_d(1+\cos\theta) + 0.5I_h\rho_g(1-\cos\theta)] \quad (18)$$

Hence

$$S = S_b + S_d \quad (19)$$

Knowing the horizontal radiation, I_h, under a clear sky, sky diffuse radiation, I_d, can be estimated by the method suggested by Liu and Jordan (1960) as follows:

$$I_d = (0.271I_0 - 0.2939I_b)\cos\theta_z \quad (20a)$$

Substituting $I_b = (I_h - I_d)/\cos\theta_z$ into the above equation obtains

$$I_d = 0.3838I_0 \cos\theta_z - 0.4162I_h \quad (20b)$$

where I_0 is the solar intensity on an extraterrestrial surface normal to the solar rays, determined by the day of the year. After obtaining the temperature distribution on the DR at any moment by solving Eqs. (1)–(6), the heat flux through the DR into the building can be calculated by

$$q_d = h_{in}[(T_{in,t} - T_i)dA_d^{(3)} + r_{in}^2 \int\int (T_{in} - T_i)\sin\theta\, d\theta\, d\phi]/A, \quad (\theta_c < \theta < \theta_0,\ 0 < \phi < 2\pi) \quad (21)$$

where $dA_d^{(3)} = \pi(r_{in}\sin\theta_c)^2$ is the area of the internal surface of the DR within $\theta < \theta_c$. The daily heat flow through the DR into the building is calculated by

$$Q_d = dt \sum_t q_d \quad (22)$$

where dt is the time step for numerical calculations.

2.2. Heat transfer through a vaulted roof (VR)

As shown in Fig. 4, a VR with average radius R, half rim angle θ_0, and vault length L is oriented with orientation ϕ_v, measured clockwise from due south. The base area of the VR is $A = 2LR\sin\theta_0$. Thus, in the cylindrical coordinate system, the heat transfer within the VR (heat transfer along the central line of the VR is neglected) would be expressed by

$$\frac{1}{r}\frac{\partial}{\partial r}\left(kr\frac{\partial T}{\partial r}\right) + \frac{1}{r^2}\frac{\partial}{\partial\theta}\left(k\frac{\partial T}{\partial\theta}\right) = \rho C_p \frac{\partial T}{\partial t} \quad (23)$$

The boundary conditions are given by

$$-k\frac{\partial T}{\partial r}\bigg|_{r=r_{ex}} = S_v - h_{ex}(T_{ex} - T_a) - 0.5\varepsilon\sigma[(T_{ex}+273)^4 - T_{sky}^4](1+\cos\theta) \quad (24)$$

$$-k\frac{\partial T}{\partial r}\bigg|_{r=r_{in}} = -h_{in}(T_{in} - T_i) \quad (25)$$

$$\frac{\partial T}{\partial\theta}\bigg|_{\theta=\theta_0} = \frac{\partial T}{\partial\theta}\bigg|_{\theta=-\theta_0} = 0 \quad (26)$$

The initial condition is as follows:

$$T(\theta,r,t)\big|_{t=0} = T_i \quad (27)$$

where θ is the polar angle measured from the X-axis towards vector $\boldsymbol{n}_{\phi_v}$ of the vault's orientation; S_v is the solar heat absorbed per unit area at any point of the VR, calculated similarly to that of the DR described in the previous section, and the incidence angle θ_i of solar radiation on the VR can also be calculated based on Eq. (14) by replacing $\boldsymbol{n}_d$ of Eq. (14) using $\boldsymbol{n}_v$ as follows:

$$\boldsymbol{n}_v = (\cos\theta,\ -\sin\theta \sin\phi_v,\ -\sin\theta \cos\phi_v) \quad (28)$$

After obtaining the temperature distribution on the VR at any moment by solving Eqs. (23)–(26), the heat flux through the VR into the building can be calculated by

$$q_v = \frac{h_{in}r_{in}}{2R\sin\theta_0}\int_{-\theta_0}^{\theta_0}(T_{in} - T_i)\, d\theta \quad (29)$$

and the daily heat flow through the VR into the building is given by

$$Q_v = dt \sum_t q_v \quad (30)$$

2.3. Heat transfer through a flat roof (FR)

Assuming the heat transfer within the FR is one-dimensional, the heat transfer equation would be given by

$$\frac{\partial}{\partial x}\left(k\frac{\partial T}{\partial x}\right)=\rho C_{\mathrm{p}}\frac{\partial T}{\partial t} \tag{31}$$

The boundary conditions are given by

$$-k\frac{\partial T}{\partial x}\bigg|_{x=0}=S_{\mathrm{f}}-h_{\mathrm{ex}}(T_{\mathrm{ex}}-T_{\mathrm{a}})-\varepsilon\sigma[(T_{\mathrm{ex}}+273)^4-T_{\mathrm{sky}}^4] \tag{32}$$

$$-k\frac{\partial T}{\partial x}\bigg|_{x=d}=-h_{\mathrm{in}}(T_{\mathrm{in}}-T_{\mathrm{i}}) \tag{33}$$

The initial condition is as follows:

$$T(x,t)|_{t=0}=T_{\mathrm{i}} \tag{34}$$

where S_{f} is the radiation absorbed per unit area of a flat roof, and is calculated through Eqs. (11)–(19) by setting $\theta_{\mathrm{i}}=\theta_{\mathrm{z}}$. The heat flux through a unit area of a FR into the building is given by

$$q_{\mathrm{f}}=h_{\mathrm{in}}(T_{\mathrm{in}}-T_{\mathrm{i}}) \tag{35}$$

and the corresponding daily heat flow through the FR into the building is given by

$$Q_{\mathrm{f}}=\mathrm{d}t\sum_{t}q_{\mathrm{f}} \tag{36}$$

3. Methodology of numerical calculations

Unfortunately, heat transfer equations dealing with heat transfer through curved and flat roofs are almost impossible to solve by analytical methods due to the instability of solar radiation and ambient temperature. Therefore, the finite element method may be used to change these partial differential equation groups into a series of ordinary differential equations with only one argument, i.e. time, t. The finite element method used in this study is based on: (a) for the DR, taking $\theta_{\mathrm{c}}=4°$, $\delta\theta=\delta\phi=\pi/90$, $\delta r=d/3$, thus the entire DR is divided into

$$n=[(\theta_0-4)/2]\times 180\times 3+3=270(\theta_0-4)+3$$

elements (computational grid is shown in Fig. 3); (b) for the VR, taking $\delta\theta=\pi/180$, $\delta r=d/3$, so the entire VR is divided into $6\theta_0$ elements (see Fig. 4); (c) for the FR, $\delta x=d/3$; (d) the center of the external surface of any element on the roof's outer layer, the geometrical center of any element at the middle roof layer, and the center of the internal surface of the roof's inner layer are considered as thermal representatives of their corresponding elements. Elements on different layers of a roof would have different forms of the governing equations due to different boundary conditions. Detailed heat transfer equations for each finite element on the curved roofs are presented in Appendix A.

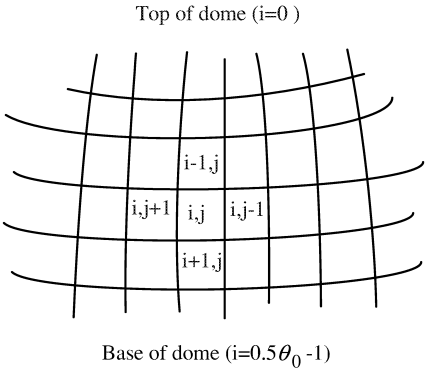

Fig. 3. Computational grid on any layer of a domed roof (DR).

By applying the computational technique of the finite difference method to each differential equation of all the finite elements and inputting the initial condition, the temperature of each finite element of the roof at any time of the day can be calculated based on climatic data, the temperature distribution of the roof at the previous moment, then regard the temperature distribution of the roof at the last moment of the day as the new initial condition. The above calculations are repeated until the relative deviation of Q between two adjacent iterant calculations is less than 0.1%. In order to ensure that numerical results converge, the time step, dt, must be very small. For the DR, when taking $\delta\theta=\delta\phi=\pi/90$, d$t$ must be less than 1 min, whereas if taking $\delta\theta=\delta\phi=\pi/180$, d$t$ must be less than 15 s. However, a comparison indicates that taking $\delta\theta$ and $\delta\phi$ as $\pi/90$ only yields less than 1% deviation of Q_{d} compared to taking $\delta\theta$ and $\delta\phi$ as $\pi/180$, but the time consumed in the numerical calculations in the latter case is 16 times that needed in the former case. To compare the

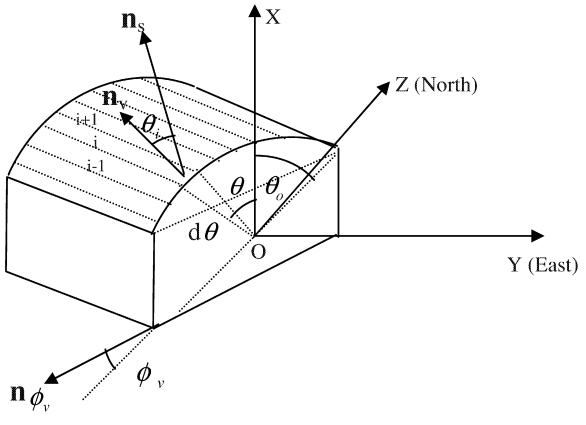

Fig. 4. Solar ray vector $\boldsymbol{n}_{\mathrm{s}}$ and normal vector $\boldsymbol{n}_{v}$ at any point of a vaulted roof (VR).

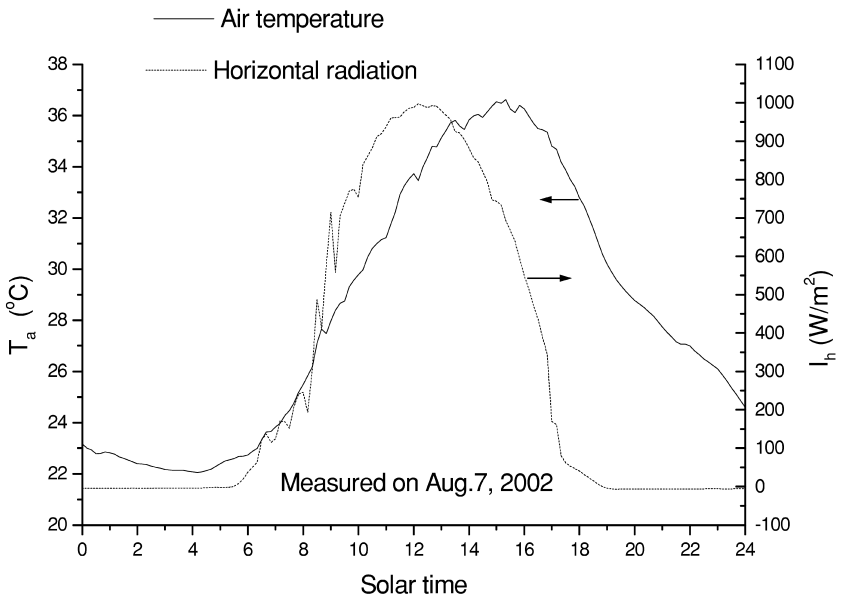

Fig. 5. Horizontal radiation and air temperature used for numerical calculations.

thermal performance between curved roofs and flat roofs, the term of daily heat flow ratio is introduced as

$$R_d = Q_d / Q_f \tag{37}$$

$$R_v = Q_v / Q_f \tag{38}$$

The climatic data used for numerical calculations, as shown in Figs. 5 and 6, are those data measured at 10-min intervals on August 7, 2002 in Sede Boqer, Israel (λ = 30.8°N), a site characterized climatically by typical hot and dry desert summer conditions. The climatic data at any moment can be obtained by the use of linear interpolation. Other parameters used for calculations are: $R = 5$ m, $d = 0.2$ m, $k = 1.4$ W/m·K, $C_p = 880$ J/kg·K, $\rho = 2300$ kg/m^3, $\alpha_n = 0.3$, $\varepsilon = 0.85$, $\rho_g = 0.2$, $T_i = 25$ °C, $h_{ex} = 9$ W/m^2·K, $h_{in} = 8.7$ W/m^2·K (Duffie and Beckman, 1991), dt = 60 s.

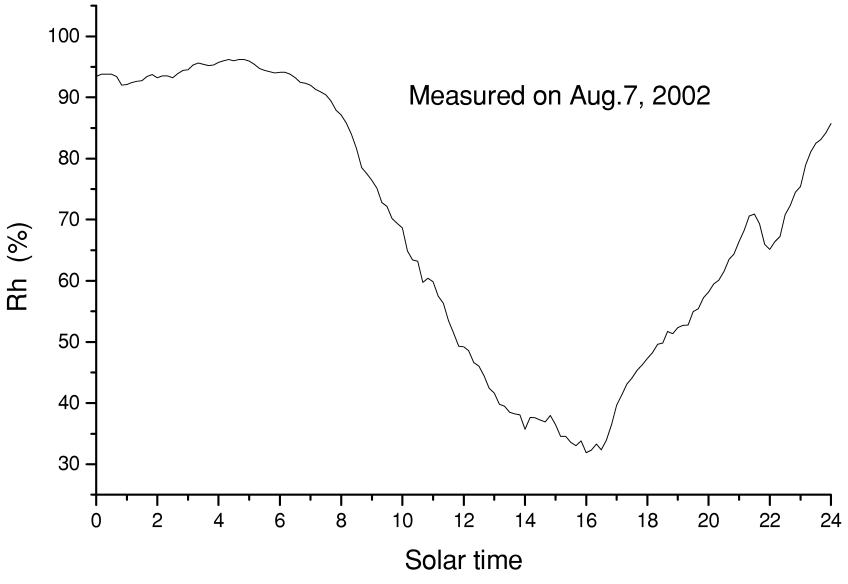

Fig. 6. Relative humidity of air used for numerical calculations.

4. Numerical results and discussion

The time variation of temperatures in a daily cycle at different points on the external surface of a DR is presented in Fig. 7. As expected, in the morning hours the eastern part of the DR maintains a higher surface temperature, whereas in the afternoon hours the western part of the DR maintains a higher temperature compared to other parts of the DR. During all hours of the daytime, the northern part of the DR stays at lower temperature, and the top of the DR keeps a higher temperature. The same pattern in the time variation of temperatures is also found on the external surface of the VR, as shown in Fig. 8.

Fig. 9 gives the time variations of heat flux through a DR, and indicates that this is always higher than that through a FR. During the morning hours, more heat flows out from the interior of the building with a DR, and during other hours more heat flows into that building. This is mainly due to the convective heat transfer between the enlarged curved roof surface and the ambient air. This can be confirmed by the effect of radiation and ambient air temperature on the daily heat flow ratio. As seen in Table 1, radiation I_h has a negligibly negative effect, but ambient temperature T_a has a very strong positive effect on the daily heat flow ratio. In other words, convective heat transfer between curved roofs and ambient air dominates their daily heat flow ratio. Such is also the situation encountered in the case of a VR, as shown in Figs. 10 and 11. As may be seen in Figs. 9–11, the half rim angle θ_0 of both the DR and the VR has a significant effect on the heat flux and the daily heat flow ratio. However, when $\theta_0 < 50°$, the heat flux through curved roofs approaches that through flat ones. This means that an appropriately designed curved roof should have a half rim angle less than 50°.

As found in a previous study by Tang et al. (2003), curved roofs absorb almost the same amount of beam radiation as flat ones (a DR absorbs slightly more beam radiation compared to a FR), but absorb more sky diffuse radiation as compared to a FR. This means that sky diffuse radiation plays a decisive role in the contribution of the total radiation absorbed by curved roofs as compared to a flat one. Combining the contribution of radiation absorbed by curved roofs and the effect of ambient temperature T_a on the daily heat flow ratio, the conclusion can be drawn that curved roofs are not suitable for areas with intense sky diffuse radiation and high ambient temperatures, such as are typical of hot humid regions. However, such roofs are suitable for areas with intense total radiation but low intensity sky diffuse radiation, such as are typical of arid regions.

Fig. 12 shows the effect of the orientation, ϕ_v, of a VR on the daily heat flow ratio, R_v. It is clear that the orientation ϕ_v of a VR with half rim angle $\theta_0 = 90°$ has some degree of influence on the daily heat flow through

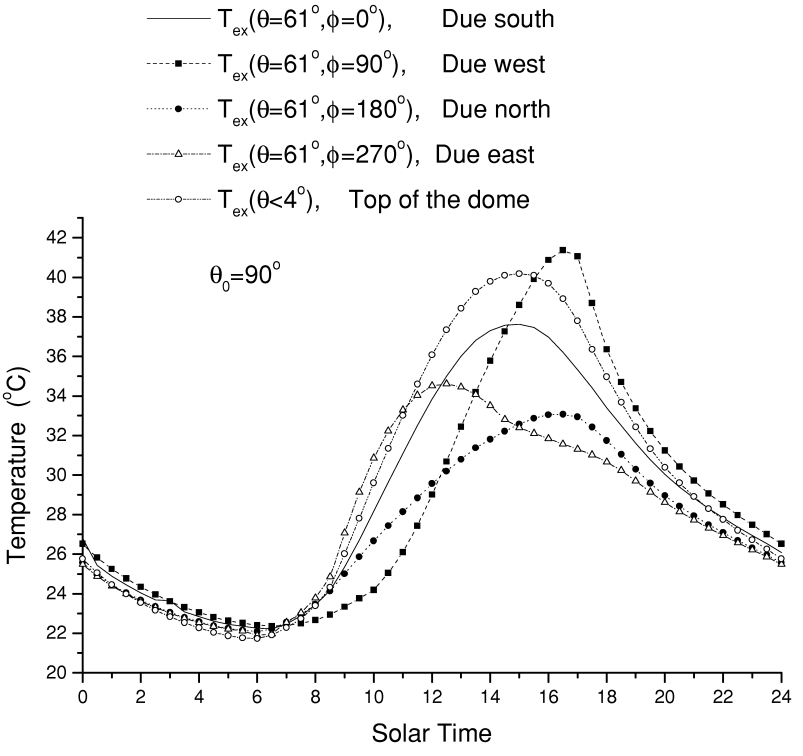

Fig. 7. Temperature variation with time at different points of a domed roof (DR).

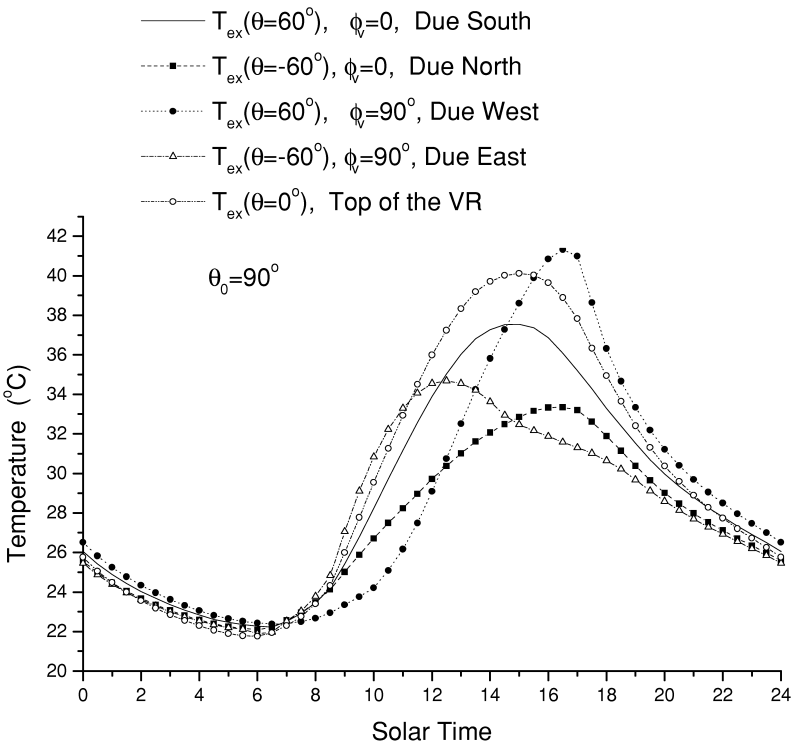

Fig. 8. Temperature variation with time at different points of a vaulted roof (VR).

the roof. A south–north oriented vault has the smallest daily heat flow ratio R_v, but with decreasing half rim angle θ_0, this effect becomes negligible. Thus, a building with a VR should be oriented as close as possible towards south–north. Fig. 13 presents the effect of the solar absorptance of the external surface of curved roofs on the daily heat flow ratio, and shows that the higher the absorptance of curved roofs, the lower the daily heat flow ratio. This

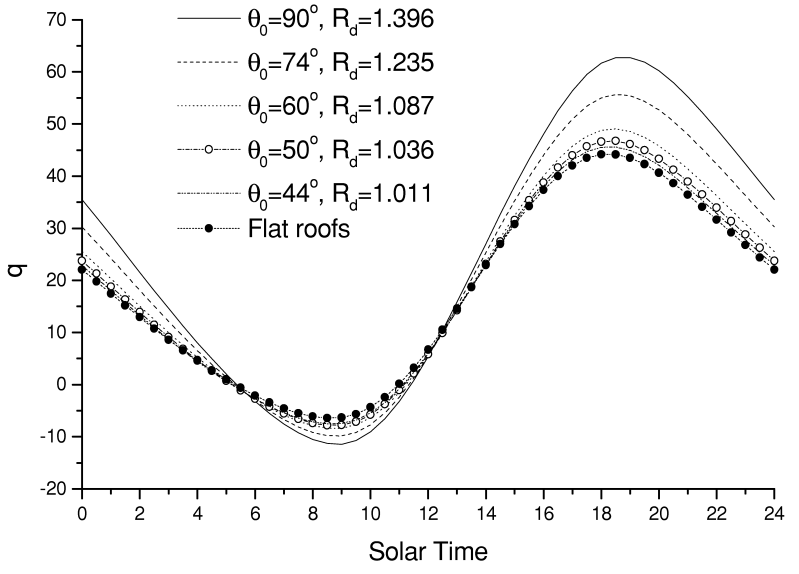

Fig. 9. Heat flux through a domed roof (DR) in a daily cycle.

Table 1
Effect of climatic conditions on the daily heat flow ratio (I_h and T_a are given by Fig. 5, $\theta_0 = 90°$)

Changed item	R_d	R_v ($\phi_v = 0$)
Horizontal radiation		
$1.2I_h$	1.368	1.149
$1.1I_h$	1.38	1.168
I_h	1.396	1.192
$0.9I_h$	1.415	1.222
$0.8I_h$	1.44	1.259
Ambient temperature		
$1.1T_a$	1.572	1.31
T_a	1.396	1.192
$0.9T_a$	0.801	0.793

result may seem strange at first glance, but can be easily explained by the fact that curved roofs with higher solar absorptance will lead to a higher surface temperature and more energy will be lost by convection and thermal radiation from the enlarged curved roof surface compared with flat ones, as observed experimentally by Pearlmutter (1993).

The high thermal stratification inside the space under a curved roof is one of the most important advantages of this roof type. The air heated by a curved roof is almost totally concentrated under the roof, in a space non-existent in a flat roof building with identical floor to roof height. This heated air can be easily exhausted by natural ventilation through openings located on the top of curved roof gable walls (Koita, 1981). Thus, compared to flat roofs, it is obvious that an appropriately designed curved roof ($\theta_0 < 50°$, $\phi_v = 0°$) would have energy savings advantages in air-conditioned buildings in hot arid areas.

Table 2 shows the effect of the ratio R/d on the daily heat flow ratio, and it indicates that the daily heat flow ratio increases slightly with increasing R/d ratio, but this comes to a halt when $R/d > 50$. This means that the daily heat flow ratio is almost unaffected by the ratio R/d. Table 3 summarizes the effect of the thermal properties of roofs on the daily heat flow ratio. It shows that the thermal diffusivity of roofs has a negligible effect on the daily heat flow ratio, but increasing the roof's thermal conductivity will gradually decrease the daily heat flow ratio. This can be explained by the fact that when the thermal conductivity of the roof is very high, it enhances the transfer to the interior of the building of the solar radiation absorbed by the roof. Compared to this heat flux, the contribution of convective heat exchange between the roof and the ambient air (a decisive factor for the heat flow ratio as discussed previously) to the total heat flux becomes smaller. However, this effect is still small in relation to that of the half rim angle.

5. Conclusions

The results of numerical calculations under typical hot dry climatic conditions show that the heat flux and the daily heat flow through curved roofs are almost unaffected by the roof radius, thickness and thermal properties, but are significantly influenced by the half rim angle of both DRs and VRs, and the ambient temperature T_a. Numerical results also indicate that the heat flux through curved roofs

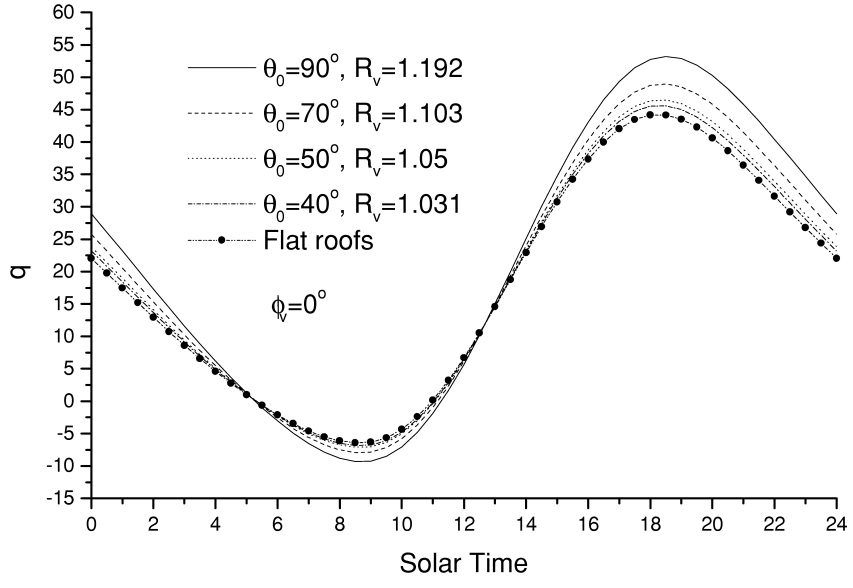

Fig. 10. Heat flux through a south–north facing vaulted roof (VR) in a daily cycle.

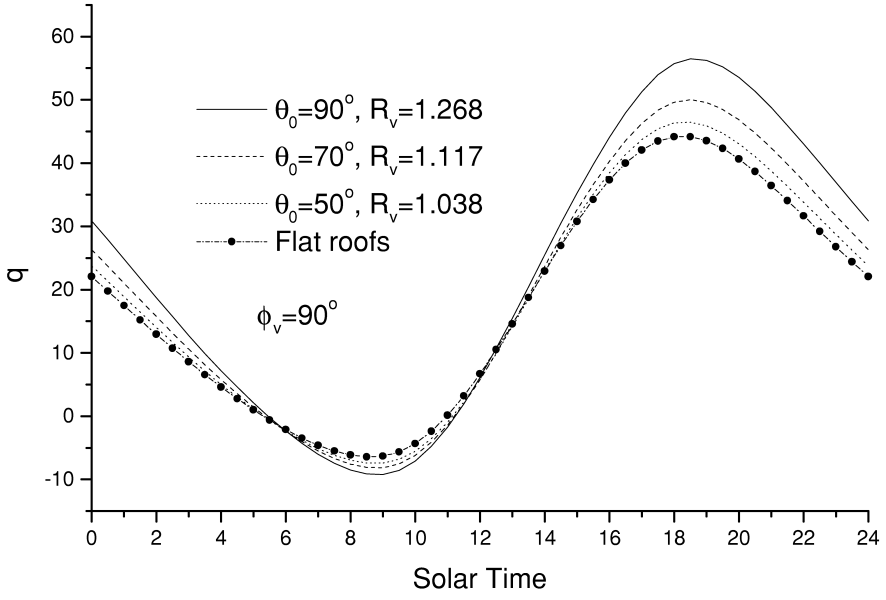

Fig. 11. Heat flux through an east–west facing vaulted roof (VR) in a daily cycle.

is always higher than that through flat ones, i.e. during the morning hours more heat flows out from the interior of the building and during other hours more heat flows into the building. Under typical hot dry climatic conditions, the daily heat flow through a DR of $\theta_0 = 90°$ is about 40% higher than that through a flat one, whereas the daily heat flow through a south–north oriented and an east–west oriented vault of $\theta_0 = 90°$ is about 20 and 27% higher than that through a flat roof, respectively. This is mainly due to the convective heat transfer between the enlarged curved roof surface and the ambient air. However, when $\theta_0 < 50°$, the heat flux and daily heat flow through curved roofs are almost identical to those through flat ones. A building with a VR should be oriented towards south–north so as to

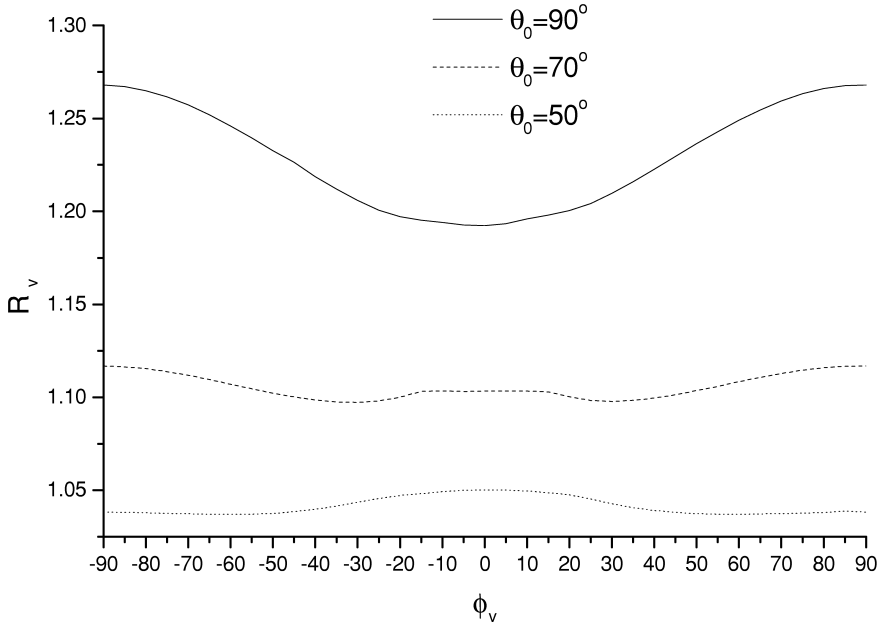

Fig. 12. The effect of the orientation of the vault on the daily heat flow ratio.

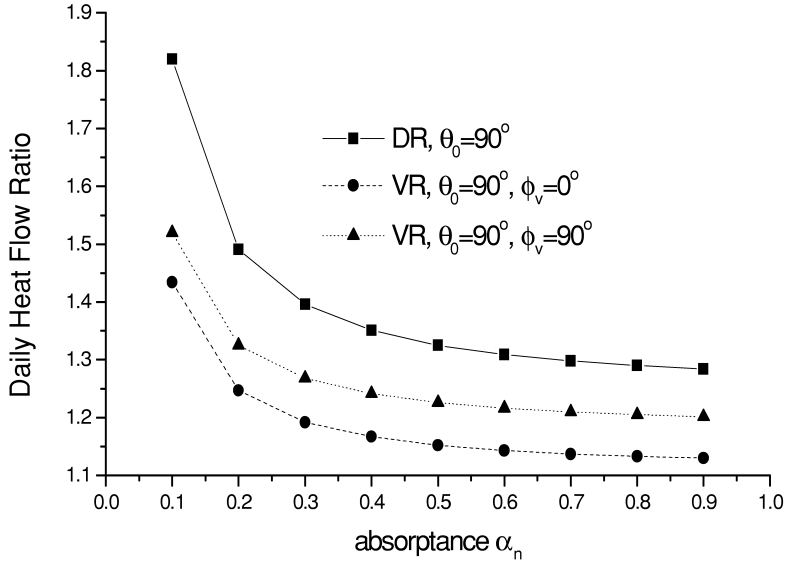

Fig. 13. Effect of the solar absorptance of the roof surface on the daily heat flow ratio.

Table 2
Effect of curve radius ($\theta_0 = 90°$) on the daily heat flow ratio

R/d	R_d		R_v ($\phi_v = 0$)	
	$d = 0.2$	$d = 0.3$	$d = 0.2$	$d = 0.3$
5	1.363	1.371	1.174	1.179
10	1.372	1.382	1.186	1.19
20	1.389	1.395	1.191	1.194
30	1.4	1.402	1.192	1.195
50	1.403	1.404	1.194	1.196
100	1.404	1.405	1.194	1.196

Table 3
Effect of the thermal properties of roofs ($\theta_0 = 90°$) on the daily heat flow ratio

Changed item	R_d	R_v, $\phi_v = 0$
μ ($k = 1.4$)		
0.5	1.396	1.192
1	1.398	1.193
2	1.4	1.194
3	1.402	1.195
5	1.403	1.195
10	1.403	1.195
k ($\mu = 1$)		
0.5	1.404	1.204
1	1.392	1.197
2	1.381	1.189
5	1.371	1.179
10	1.355	1.165
20	1.341	1.15

reduce the heat gains through the roof. The results also confirm that curved roofs are not suitable for areas with higher air temperatures and intense sky diffuse radiation typical of hot humid zones. Compared to a flat roof, curved roofs can be more energy efficient under hot arid climatic conditions if they are appropriately designed architectonically (with an opening for natural ventilation near the top) and geometrically ($\theta_0 < 50°$, $\phi_v = 0°$). The mathematical model suggested here allows comparison between the thermal behavior of curved and flat roofs in terms of heat flux and daily heat flow through the roofs into an air-conditioned building under different climatic conditions. However, the effect of a curved roof on the indoor temperature of a passive building has not been taken into account in this model due to the complexity of heat transfer between curved roofs and the indoor air.

Acknowledgements

The Avdat Roman bathhouse photo in Fig. 1 was used with the kind permission of D. Pearlmutter.

Appendix A

Energy equations for finite elements on a DR

(a) For the external layer of a DR, the energy equation for the top element would be

$$[S_t - \varepsilon\sigma[(T_{ex,t}+273)^4 - T_{sky}^4] - h_{ex}(T_{ex,t}-T_a)]dA_d + c_1(T_{m,t}-T_{ex,t})dA_d^{(1)} + D_1\sum_{j=1}^{180}[T_{ex}(1,j)-T_{ex,t}]dA_{1,j-0,j} = c_2(dA_d + dA_d^{(1)})dT_{ex,t}/dt \quad (1\le j\le 180) \tag{A.1}$$

where $r_1 = R + d/3$, $dA_d = \pi[(R+0.5d)\sin\theta_c]^2$, $dA_d^{(1)} = \pi[(R+d/6)\sin\theta_c]^2$, $dA_{1,j-0,j} = \delta r r_1 \sin\theta_c\delta\phi$, $c_1 = 2k/d$, $c_2 = \rho C_p d/6$, $D_1 = k/(r_1\sin(\theta_c+1))$, and subscript m denotes the middle roof layer. For any element (i,j) on this layer, the heat transfer equation would be

$$\begin{aligned}&[S_{ij} - 0.5\varepsilon\sigma[(T_{ex}(i,j)+273)^4 - T_{sky}^4](1+\cos\theta) - h_{ex}(T_{ex}(i,j)-T_a)]dA_{ij} + c[T_m(i,j)-T_{ex}(i,j)]dA_{ij}^{(1)}\\ &+ E_1[T_{ex}(i-1,j)-T_{ex}(i,j)]dA_{i,j-i-1,j} + E_1[T_{ex}(i+1,j)-T_{ex}(i,j)]dA_{i,j-i+1,j}\\ &+ F_1[T_{ex}(i,j-1)+T_{ex}(i,j+1)-2T_{ex}(i,j)]dA_s = c_2(dA_{ij}+dA_{ij}^{(1)})dT_{ex}(i,j)/dt\\ &(1\le i\le 0.5\theta_0-2,\ 1\le j\le 180)\end{aligned} \tag{A.2}$$

where $\theta = 2i+3$, $\phi = 2j+1$, $dA_{ij} = (R+0.5d)^2\sin\theta\cos 1^o\delta\theta\delta\phi$, $dA_{ij}^{(1)} = (R+d/6)^2\sin\theta\cos 1^o\delta\theta\delta\phi$, $dA_s = r_1\delta\theta\delta r$, $E_1 = k/(r_1\delta\theta)$, $F_1 = k/(r_1\sin\theta\delta\phi)$, $T_{ex}(0,j) = T_{ex,t}$, $T_{ex}(i,0) = T_{ex}(i,180)$, $T_{ex}(i,181) = T_{ex}(i,1)$, $T_{ex}(0.5\theta_0-1,j) = T_{ex}(0.5\theta_0-2,j)$, $dA_{i,j-i-1,j} = r_1\sin(\theta-1)\delta\phi\delta r$, $dA_{i,j-i+1,j} = r_1\sin(\theta+1)\delta\phi\delta r$.

(b) For the middle layer of the DR, the heat transfer equation for the top element would be

$$c_1(T_{ex,t}-T_{m,t})dA_d^{(1)} + c_1(T_{in,t}-T_{m,t})dA_d^{(2)} + D_2\sum_{j=1}^{180}[T_m(1,j)-T_{m,t}]\delta A_{1,j-0,j} = c_2(dA_d^{(1)}+dA_d^{(2)})dT_{m,t}/dt \quad (1\le j\le 180) \tag{A.3}$$

where $r_2 = R$, $dA_d^{(2)} = \pi[(R-d/6)\sin\theta_c]^2$, $\delta A_{1,j-0,j} = \delta r r_2\sin\theta_c\delta\phi$, $D_2 = k/(r_2\sin(\theta_c+1))$. For any element (i,j) on the middle layer, the corresponding heat transfer equation would be

$$\begin{aligned}&c_1[T_{ex}(i,j)-T_m(i,j)]dA_{ij}^{(1)} + c_1[T_{in}(i,j)-T_m(i,j)]dA_{ij}^{(2)} + E_2[T_m(i-1,j)-T_m(i,j)]\delta A_{i,j-i-1,j}\\ &+ E_2[T_m(i+1,j)-T_m(i,j)]\delta A_{i,j-i+1,j} + F_2[T_m(i,j-1)+T_m(i,j+1)-2T_m(i,j)]\delta A_s\\ &= c_2(dA_{ij}^{(1)}+dA_{ij}^{(2)})dT_m(i,j)/dt \quad (1\le i\le 0.5\theta_0-2,\ 1\le j\le 180)\end{aligned} \tag{A.4}$$

where $dA_{ij}^{(2)} = (R-d/6)^2\sin\theta\cos 1^o\delta\theta\delta\phi$, $\delta A_s = r_2\delta\theta\delta r$, $\delta A_{i,j-i-1,j} = r_2\sin(\theta-1)\delta\phi\delta r$, $\delta A_{i,j-i+1,j} = r_2\sin(\theta+1)\delta\phi\delta r$, $E_2 = k/(r_2\delta\theta)$, $F_2 = k/(r_2\sin\theta\delta\phi)$, $T_m(0,j) = T_{m,t}$, $T_m(i,0) = T_m(i,180)$, $T_m(i,181) = T_m(i,1)$, $T_m(0.5\theta_0-1,j) = T_m(0.5\theta_0-2,j)$.

(c) For the internal layer of the DR, the heat transfer equation at the top element is given by

$$c_1(T_{m,t}-T_{in,t})dA_d^{(2)} + h_{in}(T_i-T_{in,t})dA_d^{(3)} + D_3\sum_{j=1}^{180}[T_{in}(1,j)-T_{in,t}]\Delta A_{1,j-0,j} = c_2(dA_d^{(2)}+dA_d^{(3)})dT_{in,t}/dt \quad (1\le j\le 180) \tag{A.5}$$

where $r_3 = R - d/3$, $dA_d^{(3)} = \pi[(R-0.5d)\sin\theta_c]^2$, $\Delta A_{1,j-0,j} = \delta r r_3\sin\theta_c\delta\phi$, $D_3 = k/(r_3\sin(\theta_c+1))$. For any element (i,j) on this layer, the corresponding heat transfer equation is expressed by

$$\begin{aligned}&c_1[T_m(i,j)-T_{in}(i,j)]dA_{ij}^{(2)} + h_{in}(T_i-T_3(i,j))dA_{ij}^{(3)} + E_3[T_{in}(i-1,j)-T_{in}(i,j)]\Delta A_{i,j-i-1,j}\\ &+ E_3[T_{in}(i+1,j)-T_{in}(i,j)]\Delta A_{i,j-i+1,j} + F_3[T_{in}(i,j-1)+T_{in}(i,j+1)-2T_{in}(i,j)]\Delta A_s\\ &= c_2(dA_{ij}^{(2)}+dA_{ij}^{(3)})dT_{in}(i,j)/dt\\ &(1\le i\le 0.5\theta_0-2,\ 1\le j\le 180)\end{aligned} \tag{A.6}$$

where $dA_{ij}^{(3)} = (R-0.5d)^2\sin\theta\cos 1^o\delta\theta\delta\phi$, $\Delta A_s = r_3\delta\theta\delta r$, $\Delta A_{i,j-i-1,j} = r_3\sin(\theta-1)\delta\phi\delta r$, $\Delta A_{i,j-i+1,j} = r_3\sin(\theta+1)\delta\phi\delta r$, $E_3 = k/(r_3\delta\theta)$, $F_3 = k/(r_3\sin\theta\delta\phi)$, $T_{in}(0,j) = T_{in,t}$, $T_{in}(i,0) = T_{in}(i,180)$, $T_{in}(i,181) = T_{in}(i,1)$, $T_{in}(0.5\theta_0-1,j) = T_{in}(0.5\theta_0-2,j)$.

Energy equations for finite elements on a VR

$$\begin{aligned}&[S_{v,i} - 0.5\varepsilon\sigma[(T_{ex}(i)+273)^4 - T_{sky}^4]\times(1+\cos\theta) - h_{ex}(T_{ex}(i)-T_a)]dA_i\\ &+ c_1[T_m(i)-T_{ex}(i)]dA_i^{(1)} + E_1[T_{ex}(i-1)+T_{ex}(i+1)-2T_{ex}(i)]dA_{sv}\\ &= c_2(dA_i+dA_i^{(1)})dT_{ex}(i)/dt \quad (1\le i\le 2\theta_0)\end{aligned} \tag{A.7}$$

$$\begin{aligned}&c_1[T_{ex}(i)-T_m(i)]dA_i^{(1)} + c_1[T_{in}(i)-T_m(i)]dA_i^{(2)} + E_2[T_m(i-1)+T_m(i+1)-2T_m(i)]dA_{sv}\\ &= c_2(dA_i^{(1)}+dA_i^{(2)})dT_m(i)/dt \quad (1\le i\le 2\theta_0)\end{aligned} \tag{A.8}$$

$$\begin{aligned}&c_1[T_m(i)-T_{in}(i)]dA_i^{(2)} + h_{in}(T_i-T_{in}(i))dA_i^{(3)} + E_3[T_{in}(i-1)+T_{in}(i+1)-2T_{in}(i)]dA_{sv}\\ &= c_2(dA_i^{(2)}+dA_i^{(3)})dT_{in}(i)/dt \quad (1\le i\le 2\theta_0)\end{aligned} \tag{A.9}$$

where $\theta = \theta_0 + 0.5 - i$, $r_1 = R + d/3$, $r_2 = R$, $r_3 = R - d/3$, $dA_i = (R+0.5d)L\delta\theta$, $dA_i^{(1)} = (R+d/6)L\delta\theta$, $dA_i^{(2)} = (R-d/6)L\delta\theta$, $dA_i^{(3)} = (R-0.5d)L\delta\theta$, $dA_{sv} = L\delta r$, $T_j(0) =$

$T_j(1)$, $T_j(2\theta_0 + 1) = T_j(2\theta_0)$ (subscript $j = 1,2,3$ denote the external, middle and internal layer, respectively).

Energy equations for finite elements on a FR

$$S_f - \varepsilon\sigma[(T_{ex} + 273)^4 - T_{sky}^4] - h_{ex}(T_{ex} - T_a) + c_1(T_m - T_{ex}) = c_2 dT_{ex}/dt \quad (A.10)$$

$$c_1(T_{ex} + T_{in} - 2T_m) = c_2 dT_m/dt \quad (A.11)$$

$$c_1(T_m - T_{in}) + h_{in}(T_i - T_{in}) = c_2 dT_{in}/dt \quad (A.12)$$

Method for numerical calculations

Assuming the time step, dt, for the numerical calculations is very small, within which the climatic parameters are regarded as constant, radiative heat exchange $\varepsilon\sigma[(T_{ex} + 273)^4 - T_{sky}^4]$ can be simplified as $4\varepsilon\sigma(T_a + 273)^3(T_{ex} - T_{sky})$, hence the energy equation for all finite elements can be changed into the following form:

$$dT/dt + C_{11}T = C_{22} \quad (A.13)$$

The solution of the above equation by use of the finite difference method is

$$T(t + dt) = e^{-C_{11}dt}(T(t) + C_{22}dt) \quad (A.14)$$

where $T(t)$ is the temperature at the previous moment, and C_{11} and C_{22} are constants determined for a given moment by the governing energy equation of each finite element.

References

Bahadori, M.N., 1978. Passive cooling systems in Iranian architecture. Sci. Am. 238 (2), 144–154.

Berdahl, P., Fromberg, R., 1982. The thermal radiance of clear skies. Solar Energy 29, 299–314.

Bowen, A.B., 1981. Cooling achievement in the gardens of Moghul India. In: Proceedings of the International Passive and Hybrid Cooling Conference, Miami Beach, FL, pp. 27–31.

Cook, J., 1985. Passive Cooling. MIT Press, Cambridge, MA.

Duffie, J.A., Beckman, W.A. (Eds.), 1991. Solar Engineering of Thermal Processes, 2nd Edition. Wiley, New York, p. 209.

Fathy, H. (Ed.), 1973. Architecture for the Poor. University of Chicago Press, Chicago, pp. 5–12.

Fathy, H. (Ed.), 1986. Natural Energy and Vernacular Architecture. University of Chicago Press, Chicago, p. 50.

Incropera, F.P., Dewitt, D.P., 1996. Fundamentals of Heat Transfer. Wiley, New York.

Koita, Y., 1981. Comfort attainment in Moghul architecture. In: Proceedings of the International Passive and Hybrid Cooling Conference, Miami Beach, FL, pp. 32–36.

Liu, B.Y., Jordan, R.C., 1960. The interrelationship and characteristic distribution of direct, diffuse, and total solar radiation. Solar Energy 4, 1.

Mainstone, R.J. (Ed.), 1983. Developments in Structural Form. MIT Press, Cambridge, pp. 95–136.

Olgyay, V. (Ed.), 1973. Design with Climate, 2nd Edition. Princeton University Press, Princeton, p. 7.

Pearlmutter, D., 1993. Roof geometry as a determinant of thermal behavior: a comparative study of vaulted and flat surfaces in a hot-arid zone. Architect. Sci. Rev. 36 (2), 75–86.

Rabl, A. (Ed.), 1985. Active Solar Collectors and Their Applications. Oxford University Press, New York, pp. 65–68.

Tang, R.S., Meir, I.A., Etzion, Y., 2003. An analysis of absorbed radiation by domed and vaulted roofs as compared with flat roofs. Energy and Buildings 35 (6), 539–548.